Ensemble hindcasting of wind and wave conditions with WRF and Wavewatch III® driven by ERA5

Robert Daniel Osinski[1] and Hagen Radtke[1]

[1]Leibniz Institute for Baltic Sea Research Warnemünde, Seestrasse 15, 18119 Rostock, Germany

Correspondence: Robert Daniel Osinski (robert.osinski@io-warnemuende.de)

Abstract. When hindcasting wave fields of storm events with state-of-the-art wave models, the quality of the results strongly depends on the meteorological forcing dataset. The wave model will inherit the uncertainty of the atmospheric data, and additional discretisation errors will be introduced due to a limited spatial and temporal resolution of the forcing data. In this study, we demonstrate that applying an atmospheric downscaling with the atmospheric mesoscale model WRF can address all these three issues. Not only does it add regional detail to the wind field and can increase the temporal resolution of the wind fields, which gives a more detailed representation of transient events such as storms. It can also be used to generate ensembles with perturbed atmospheric conditions which allow for a flow dependent and spatiotemporally variable uncertainty estimation. We test different strategies to generate an ensemble hindcast of a storm event in February 2002 in the Baltic Sea, which provoked a severe storm surge. The WRF model used for this purpose is driven by the ECMWF ERA5 reanalysis, and wind fields are passed to the third-generation wave model Wavewatch III®. A combination of initial conditions from the ERA5 ensemble of data assimilations and stochastic pertubations during runtime is identified as the most promising strategy. The final aim of the ensemble approach is to quantify the hindcast error, but this approach can also be used to generate alternative representations of historical extreme events to sample the recent climate and to increase the sample size for statistical studies, such as for civil engineering applications for coastal protection studies.

1 Introduction

The Lorenz attractor (Lorenz, 1963) is often used as an example to motivate ensemble forecasts. It explains a chaotic system behaviour, which is very sensitive to slight differences in the initial conditions and it is described by a system of differential equations. In operational weather prediction, ensemble forecasts are a common tool to quantify the forecast uncertainty by producing a set of alternative realisations. Initial conditions are estimated by data assimilation combining observations with a background field, which is normally a previous model run. The sparse spatiotemporal observational coverage leads to uncertainties in the initial conditions, which are growing over the integration time. A second type of uncertainty comes from the model parametrisations. These are used to take processes into account, which cannot be resolved by the dynamical core of the model, e.g. subgrid-scale processes like turbulence or convection or processes which can be described physically but are computationally too expensive to explicitly take them into account (e.g. utilisation of a 1-moment instead of a 2-moment micro physics scheme). In principle, three methods exist to generate an ensemble forecast. Some of them are tested to estimate the

uncertainty of a hindcast. One possibility is the combination of forecasts from different models (e.g. Hagedorn et al., 2005) or using the same model with different types of model physics (e.g. Ricchi et al., 2019). This multi-model/physics approach has the disadvantage that the ensemble size is limited to the number of available models/physics packages. Also, the forecast skill over a specific region and a specific variable might differ between the different models, what has to be taken into account in

5 the interpretation. A second approach is the combination of forecast runs from the same model for the same time instance, but started at different initialisation times, called lagged-average forecast (LAF) ensemble (Hoffman and Kalnay, 1983). A limitation here is also the number of forecasts covering the same time instance and the fact that a newer forecast can be expected to have in average a better forecast skill than a forecast at long lead times. The third method is the utilisation of a single model and applying pertubations to the initial conditions and/or to the model physics. Such an approach is used operationally at the

10 European Centre for Medium-Range Weather Forecasts (ECMWF) since 1992. Initial conditions are perturbed by singular vectors (Buizza, 1998) or by a combination of Ensemble data assimilation (Buizza et al., 2008) with singular vectors, or by breeding vectors (Toth and Kalnay, 1997) like in case of the National Centers for Environmental Prediction (NCEP). Stochastic perturbations like Stochastically Perturbed Parametrization Tendencies (SPPT) (Buizza et al., 1999), Stochastically Perturbed Parametrizations (SPP) (Ollinaho et al., 2017) and Stochastic Kinetic Energy Backscatter (SKEB) (Shutts, 2005) are used to

15 perturb the model physics (Leutbecher et al., 2016, 2017). SPPT perturbs the model parametrizations by applying a multiplicative noise and SKEB simulates the upscale transfer of kinetic energy from smaller to larger scales. Besides the application of SPPT in the global ECMWF medium-range ensemble system, stochastic perturbations are also used in local area models (e.g. Bouttier et al., 2012) and in ocean models like in NEMO (e.g. Brankart et al., 2015).

In a well constructed ensemble, the ensemble spread reflects the average forecast error. Stochastic perturbations need some

20 time until a reasonable spread develops. Ensemble data assimilation (EDA) gives different estimations of the initial state representing its uncertainty. A forecast started from the different members develops the desired ensemble spread faster.

ERA5 (Copernicus Climate Change Service (C3S), 2017) is the newest global reanalysis from ECMWF. The resolution is relatively high with about 31 km resolution for the atmospheric variables, but depending on the application, it can be still too coarse. From ERA5, in contrast to previous reanalyses, an uncertainty measure based on an ensemble of data assimilation is

25 available.

The Weather Research and Forecasting (WRF) (Skamarock et al., 2019) model is widely used in research as well as in operational weather forecasting and includes implementations of the mentioned stochastic perturbation schemes. The motivation of driving WRF with this new dataset is to be able to produce hindcasts of atmospheric conditions in different spatiotemporal resolutions including a measure of uncertainty based on ensemble techniques. This allows for example to study the effect of

30 the model resolution on effects like up- and downwelling in coastal regions.

Some regional reanalysis (ensemble) datasets are already freely available. Such regional reanalyses are produced, for example, in the framework of the project "Uncertainties in Ensembles of Regional ReAnalysis" (UERRA)[1]. The ensemble datasets in this project cover at the moment only short periods or have a coarse resolution, why it can be advantageous to be able to produce hindcasts of events during a longer period, allowing also to adapt the spatiotemporal resolution to the needs. It has to

[1]http://www.uerra.eu/

be mentioned that the quality of a freely running hindcast can be expected to be inferior to such a re-/analysis product containing state-of-the art data assimilation techniques. Another database from which ensemble forecasts of local area models are available is from the Tigge-LAM archive[2] (Swinbank et al., 2016). The available forecast models cover also only short periods and they are operational, meaning that the datasets are not homogeneous, because the model version can change during time.

5   The idea behind this study is to generate an ensemble hindcast on event basis in a comparable way to operational weather forecasts by driving WRF with ERA5 including the initial conditions from the ERA5 EDA with stochastic perturbations (SKEB and SPPT). Other ensemble generation techniques are tested for comparison. The atmospheric data from a hindcast or forecast are discrete in time and space. This limits the accuracy and affects the outcome if driving another model like an ocean or wave model. This uncertainty is investigated by driving a wave model with different spatiotemporal resolutions.

2   Data and models

2.1   Data

2.1.1   ERA5

ERA5[3] (Copernicus Climate Change Service (C3S), 2017) is the follow-up ECMWF reanalysis of ERA-Interim produced with the Integrated Forecasting System (IFS) cycle 41R2[4], operationally at ECMWF in March 2016. It is provided under the Copernicus licence[5] allowing also commercial applications. Hourly reanalysis in about 31 km (∼0.28°) horizontal resolution and 137 vertical model levels are available from 1979 (eventually 1950) and the dataset is getting prolongated into the future with a delay of about three months. A state-of-the-art data assimilation technique is used (4D-Var). Additionally to the reanalysis, on three hourly basis ten members of an ensemble of data assimilation (EDA) are provided as an uncertainty measure with half the resolution of the reanalysis. The reanalysis data of surface fields and the 137 model levels were extracted on hourly basis interpolated onto a slightly higher 0.25° resolution grid for the period 21. February 2002 until 24. February 2002 as recommended by ECMWF. ERA5 data from the ensemble of data assimilation were also interpolated bilinearly onto the same 0.25° regular longitude-latitude grid. ERA5 also includes fields from the ECWAM wave model (ECMWF, 2016) in 0.36° and in 1° from the ensemble of data assimilation. The ERA5 dataset was used in this study to drive the atmospheric model WRF, a coarse Wavewatch III® wave model to provide lateral boundary conditions for a Wavewatch III® wave model with higher resolution and for comparison with the model results.

2.1.2   UERRA/Harmonie-v1

The UERRA/Harmonie-v1 dataset (Ridal et al., 2017) contains analyses at 00, 06, 12 and 18 UTC as well as hourly forecasts for +1h until +6h and thereafter three hourly until thirty hours. The Harmonie model is used for the production of this dataset

---

[2]https://apps.ecmwf.int/datasets/data/tigge-lam/expver=prod/type=pf/

[3]https://confluence.ecmwf.int/display/CKB/ERA5+data+documentation

[4]https://www.ecmwf.int/en/forecasts/documentation-and-support/changes-ecmwf-model/ifs-documentation

[5]http://apps.ecmwf.int/datasets/licences/copernicus/

in about 11 km horizontal resolution and 3D-Var data assimilation is used with conventional observations (synoptic stations, ships, drifting buoys, aircraft observations and radio soundings). Large scales from ERA40 and ERA-Interim are introduced into the data assimilation by large scale mixing. The available period extends back until 1961. To create an hourly dataset, the analysis fields were combined with the forecast lead times +1h to +5h, retrieved from ECMWF[6]. Wind data were interpolated

5   bilinearly onto the regular wave model grid for the Baltic Sea described in the next section. This dataset was mainly used to produce a restart file for the wave model runs and for calibration/validation of the wave model.

2.2   Models

2.2.1   Atmospheric Weather Research and Forecasting model (WRF)

The Weather Research and Forecasting model WRF v4.0.3 model[7] in the Advanced Research WRF (ARW) (Skamarock et al.,

10   2019) version is applied here. It is used in non-hydrostatic mode in 0.126° horizontal resolution writing 15 minutes output. To investigate the impact of different horizontal resolutions on the significant wave height, runs in 0.252°and 0.063° were produced as well as output at a temporal resolution of 5 minutes to investigate the temporal impact. In this way, a factor of about 4.5 between the highest WRF resolution and the driving ERA5 fields is given, and the same factor between the ERA5 EDA fields and the WRF ensemble runs. The domain is slightly larger than the Baltic Sea for all runs. For the model configuration, the

15   CONUS physics suite (Wang et al., 2019) is used. This is a combination of model physics adapted for the Continental United States of America. As it is well tested, this physics setup is taken as it is, and we assume that it should be reasonable for other regions in the mid-latitudes. The 89 vertical Eta layers used in this WRF setup are adapted to be comparable to layer 2 to 90 of the IFS[8] until 50 hPa. As initial conditions come from a different and coarser model, it needs some time until fine scales develop. Methods for spin-up reduction like Digitial Filter Initialisation (Peckham et al., 2016) have not been tested. Instead,

20   the WRF output is only used twelve hours after initialisation to drive the wave model. Neither data assimilation nor observation nudging is used. Hindcasts are produced in this study in a comparable way like a forecast, downscaled from a global forecast model. For this reason, the results of this study are valid for both hindcasts and such forecasts. The WRF Pre-Processing System (WPS) in version 4.0.3 is used to prepare the input data for the model together with the WPS V4 Geographical Static Data[9].

25   ### 2.2.2   Wave model Wavewatch III®

Wavewatch III v6.07® [10] (Tolman, 1991; The WAVEWATCH III® Development Group (WW3DG), 2019) is used in this study for the Baltic Sea. It is a state-of-the art third generation wave model, which is also used as an operational wave forecast model. A one-way nesting approach is applied, see figure 1: A setup with 0.1° resolution covering the North Sea and a small part of

---

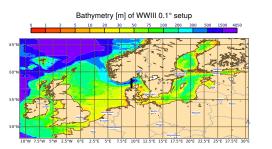[6]https://apps.ecmwf.int/datasets/data/uerra

[7]https://github.com/wrf-model/WRF/releases

[8]https://www.ecmwf.int/en/forecasts/documentation-and-support/137-model-levels

[9]http://www2.mmm.ucar.edu/wrf/src/wps_files/geog_high_res_mandatory.tar.gz

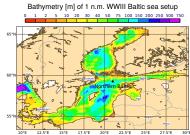[10]https://github.com/NOAA-EMC/WW3

Figure 1. Bathymetries [m] and domains of 0.1° and 1 nautical mile Wavewatch III® setups; black points in left panel show grid cells for the nesting of the Baltic Sea model. The black point in the right panel shows the location of timeseries for figure 6

the eastern Atlantic ocean is used to produce boundary conditions for the Baltic Sea setup at the border with the North Sea. The GEBCO_2014 Grid in version 20150318[11] is used as bathymetry. The Baltic Sea setup has a resolution of one nautical mile with 149.282 sea grid points and the bathymetry is based on the work of Seifert et al. (2001). UERRA/Harmonie-v1 was used for calibration and validation of the setup against one month of data from buoys available from the Copernicus Marine

5   environment monitoring service[12] (CMEMS) with the previous Wavewatch III v5.16 version. A calibration and validation with the WRF forcing was not yet possible because of the short period that has been hindcasted until now. 24 directions starting at 7.5° with a 15° direction increment and 30 frequencies starting at 0.03453 Hz geometrically distributed with a step of 1.1 are used for the discretisation of the energy spectrum. This is comparable to the settings for the wave model in ERA5. The physics packages are defined before compiling the model by a so-called switch file. The switch file Ifremer1, provided with the model

10 code, is applied in this study. This includes wind input and dissipation after Ardhuin et al. (2010) and the SHOWEX bottom friction scheme (Ardhuin et al., 2003). A sediment map based from the European Marine Observation and Data Network EMODnet[13] data were used for applying non-homogeneous bottom friction. The model runs were produced between 2002-02-22 00UTC and 2002-02-24 00UTC. Wavewatch III® was started from initial conditions from a previous run conducted over 21 days driven with UERRA/Harmonie-v1. The sea ice area fraction is taken from ERA5. Wave models include different

15 source terms (e.g. wave generation, dissipation, bottom-friction, and so on), which are partly simplified to make the model computationally more efficient or are described empirically (Farina, 2002; Yildirim and Karniadakis, 2015). Nevertheless, the ensemble approach here is based solely on the ensemble of the atmospheric forcing data and includes no perturbations of the source terms.

---

[11] http://www.gebco.net

[12] http://marine.copernicus.eu/services-portfolio/access-to-products/?option=com_csw&view=details&product_id=INSITU_BAL_NRT_ OBSERVATIONS_013_032

[13] http://www.emodnet-geology.eu/

Ocean Science
Discussions

3 Ensemble hindcasts

3.1 Wind fields

Six different approaches to generate an ensemble hindcast are presented in this section. The first approach is to generate an LAF ensemble. This is done by initialising the WRF model at different times on 21. February 2002 at every hour between
5 08 and 16 UTC, which results in 9 runs covering the period from 22nd to 24th of February. The second approach is based on the domain shifting presented by Pardowitz et al. (2016). The ERA5 reanalysis is for this purpose shifted by one grid cell (0.25°) in each direction horizontally producing 8 perturbed ensemble members. For the third approach, WRF is initialised from the ERA5 fields from the ensemble of data assimilation. These fields have a coarser resolution, but they are used in this study as the ERA5 reanalysis in 0.25°. This has the disadvantage that finer scales are not represented, but this is comparable
10 to a downscaling from a global ensemble model, except that the reanalysis is used here as lateral boundary condition. As an alternative to keep the finer scales, it was tested to add perturbations to the initial fields, calculated by the difference between the ERA5 EDA members and the EDA ensemble mean, once with positive and negative sign to the ERA5 HRES reanalysis. We didn't find an improvement against the direct application of the ERA5 EDA fields. SKEB and SPPT are used for the fourth approach and the fifth combines approach three and four. For approach six, the same setup is used as in approach five, but
15 as the ERA5 EDA fields are available every three hours, runs three hours earlier and later are additionally used as in an LAF approach. This leads to a thirty member ensemble.

    In an ensemble system, it is important that the ensemble spread reflects the uncertainty. If the spread is too narrow, the system is underdispersive meaning that the forecast is overconfident and vice versa for an overdispersive/underconfident forecast. One tool for quantifying the quality of the ensemble spread is, for example, the Talagrand (rank) diagram (Hamill, 2001), and
20 there are other quality measures like for example reliability, resolution, accuracy or sharpness, which are important for a good ensemble system (Murphy and Winkler, 1992). To be able to use the traditional ensemble verification methods (Jolliffe and Stephenson, 2003), long time series are needed, which could not be produced in this study. For this reason, an absolute statement which of the tested approaches performs best can not be given based on only one single hindcasted event. The different approaches are compared against the ERA5 reanalysis and the ERA5 members from the ensemble of data assimilation.
25 As a larger variability can be expected in the higher-resolution model, it can be assumed that it increases also the uncertainty, what should be reflected by a larger spread than found in the much coarser data from the ERA5 ensemble of data assimilation.

    A good agreement at a specific location between the ERA5 reanalysis and the WRF runs is visible during the first twenty hours in figure 2. The wind speed maximum is higher than in ERA5. For comparison, the closest grid cell of the UERRA/Harmonie-v1 data is plotted and also shows higher values than ERA5. From ERA5, also the wind speed from the closest grid cell of the
30 0.25° grid is plotted, why some deviations from the initial conditions, which were prepared differently with the WRF preprocessing system, are visible. The resolution of the WRF runs is closer to the one from UERRA/Harmonie-v1, and a stronger variability and also higher extremes can be expected due to the difference to the ERA5 resolution. WRF adds additional information from the finer scales and resolves the orography, coastlines and islands better.
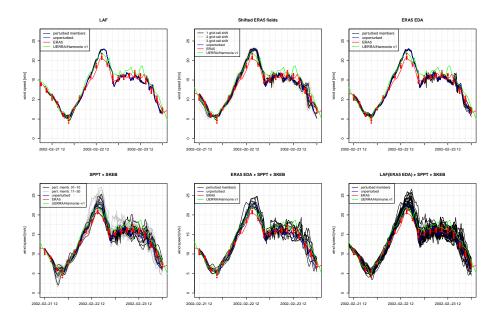
Ocean Science
Discussions

EGU

Figure 2. Time series demonstrating the simulation results of the different ensemble generation strategies at one specific location: lagged-average forecast (LAF) ensemble (Hoffman and Kalnay, 1983), domain shifting (Pardowitz et al., 2016), WRF runs started from ten ERA5 4D-EnVAR members with HRES LBC's, stochastic perturbations (SPPT and SKEB) (Buizza et al., 1999; Shutts, 2005), ERA5 4D-EnVAR as starting conditions plus stochastic perturbations, and LAF started from ERA5 4D-EnVAR at 09, 12 and 15 UTC plus stochastic perturbations; results shown at 19.39°E, 56.17°N

All ensemble techniques lead to deviations from the unperturbed run. The LAF ensemble shows a very small spread. In fact, this is good, because it means that irrespective of the starting time of the WRF model being shifted by a few hours, the outcome is comparable. The first three approaches show a lower ensemble spread than the ensembles which include stochastic perturbations. Compared to the ERA5 EDA members, it gives an indication that these ensembles could be underdispersive. During the first hours of the ensemble with only stochastic perturbations (ensemble approach 4), all members are identical, as it needs some time until the perturbations introduce spread. Starting from the ERA5 ensemble of data assimilation (ensemble approaches 3, 5, and 6), spread is visible from initialisation on. Even with the coarser resolution of theses fields, its application seems to be working, but additionally stochastic perturbations are necessary to produce a larger spread. The WRF ensemble started from ERA5 EDA fields at 09, 12 and 15 UTC also represents the uncertainty at February 21st at 21UTC, where the lowest values in the ERA5 EDA members (Fig. 2) in the shown period can be found. With only stochastic perturbations, such low values are also visible, but a few hours too early. For the last simulation day, the spread of the combined ERA5 EDA and stochastic perturbations approach is very large, but it could not be tested if it is overdispersive.

Spatially (Fig. 3), the spread in the WRF ensemble started from ERA5 EDA is very small. A much larger spatial variability is presented by applying stochastic perturbations. Especially strong wind is present in some members over the northern part of the Baltic Sea. The LAF approach also shows very little spread spatially over the entire domain. Domain shifting also did not
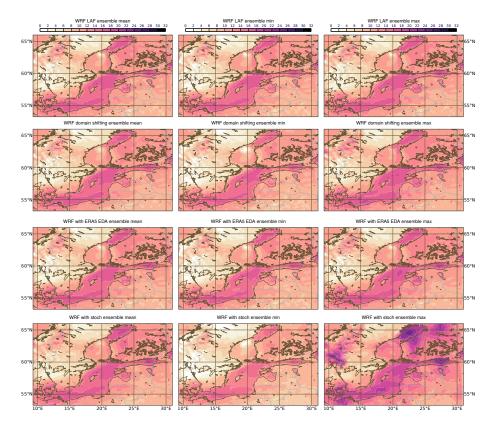
7

Figure 3. Ensemble mean, minimum and maximum wind speed [m/s] of WRF ensemble based on LAF approach, domain shifting, initial conditions from the ERA5 EDA and on stochastic perturbations. All initialised at 2002-02-21 12UTC. Shown 2002-02-23 09UTC.

produce as strong variability as applying stochastic perturbations. The combination of ERA5 EDA and stochastic perturbations produces members which show a strong variability in the central Baltic Sea (Fig. 4).

The LAF approach also shows very little spread spatially over the entire domain, and domain shifting also did not produce as strong variability as applying stochastic perturbations (Fig. 3).

5   A strong variability in the Northern as well as in the Central Baltic Sea is present by initialising WRF at 09, 12 and 15 UTC from ERA5 EDA fields with stochastic perturbations. Ten members are a small number to sample the uncertainty. Comparing a ten with a thirty member ensemble is not really a fair comparison. Ensemble approach number 6 shows in the ensemble maximum of all ensemble members high values in the central as well as in the northern part of the Baltic Sea. Figure 2 shows also the WRF ensemble with only stochastic perturbations and thirty members. The spread is in this case larger, but still inferior

10 to the thirty member approach number 6 with ERA5 EDA as initial conditions and stochastic perturbations. Also the region in the central Baltic Sea gains spread by adding additional members, but contains lower spread than in approach number 6 shown in figure 5. This demonstrates that ten members might be still not sufficient to sample the entire range of uncertainty, and that the combined application of model and initial perturbations is beneficial to create a larger spread.
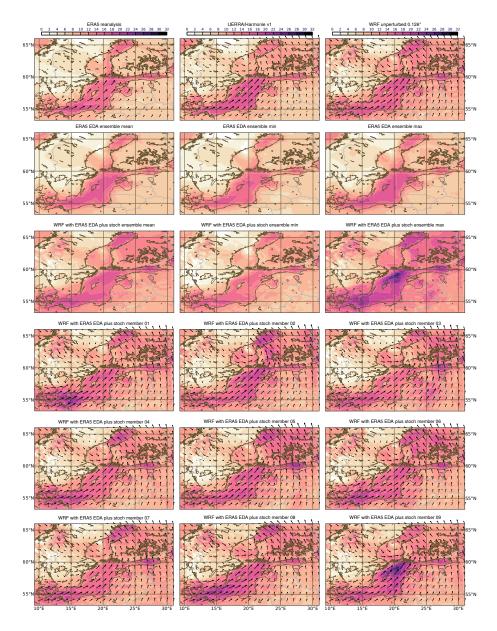
Figure 4. Postage Stamps: WRF ensemble approach number five generated by starting the ten members from ten ERA5 EDA members at 2002-02-21 12UTC plus stochastic perturbations SPPT and SKEB. Shown 2002-02-23 09UTC. The ERA5 reanalysis, ERA5 EDA ensemble mean, minimum and maximum, WRF unperturbed, WRF ensemble mean, minimum and maximum, UERRA/Harmonie-v1, and the perturbed WRF members are shown. Wind Speed [m/s] and direction as arrows.
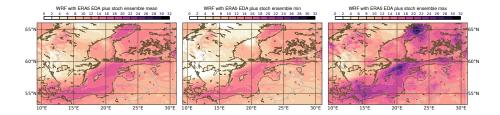
Figure 5. Ensemble mean, minimum and maximum wind speed [m/s] from WRF ensemble approach number 6 generated by starting three times ten members from ERA5 EDA members at 2002-02-21 09/12/15 UTC plus stochastic perturbations SPPT and SKEB. Shown 2002-02-23 09UTC.

3.2 Wave fields

The LAF and domain shifting approaches were not used to drive the wave model, because they show a relatively small spread. Figure 6 shows a time series at a station in the central Baltic Sea (see figure 1). The comparison with the closest grid cell from ERA5 shows a good agreement in the temporal evolution of growth and a comparable trend in the decay of the significant wave

5 height, but the maximum peak is about one metre lower in ERA5. ERA5 also shows the second peak only very weakly and some hours later during the middle of the second simulation day. Wavewatch III® in this study has a much higher resolution with 1 n.m. compared to the 0.36° ECWAM model of the ERA5 reanalysis and the WRF wind forcing is spatially (0.126° vs. 0.28°) and temporally (15' vs. 60') of higher resolution. This can explain locally much higher values and a stronger variability. Especially the maximum of the significant wave height varies strongly between the different ensemble realisations.

10 This difference can be due to a different dynamical evolution of the storm or due to different tracks in the atmospheric model members (compare Osinski et al., 2016), leading to differences in the position. Already a slight change in the track of the storm can provoke large differences in the maximum if looking at a specific location in such a high resolution. With 0.36° resolution in ERA5, a slight change in the track can be assumed to not lead to such strong differences.

Figure 7 shows the different wave model members driven by WRF with ERA5 EDA initial conditions and stochastic per-

15 turbations. All members show high values in the central Baltic Sea. The time series shown in figure 6 is in this region with the highest significant wave height on 22. February 2002 at 09 UTC. There is also a strong variability between the different ensemble members in this region. Wave heights in member 8 are especially higher than in the other members in the Gulf of Bothnia, but this member shows also much higher wave heights than the other members in the central Baltic Sea. In the western Baltic Sea the differences between the members are not that strong. Compared to ERA5, the overall spatial pattern is

20 comparable. The wave models (Fig. 6) driven by the WRF ensemble hindcast started from the ERA5 EDA initial conditions show a very small spread. A difference can be especially seen at the second peak. Much stronger differences are provoked by the WRF ensemble based on stochastic perturbations. Combining both ERA5 EDA fields as initial conditions and stochastical perturbations produces a comparable spread.

A shortcoming of this procedure is the fact that the wave model runs were all started from the same initial state. This

25 means that a certain time is needed until the different members diverge, especially as the total wave height is a combination of
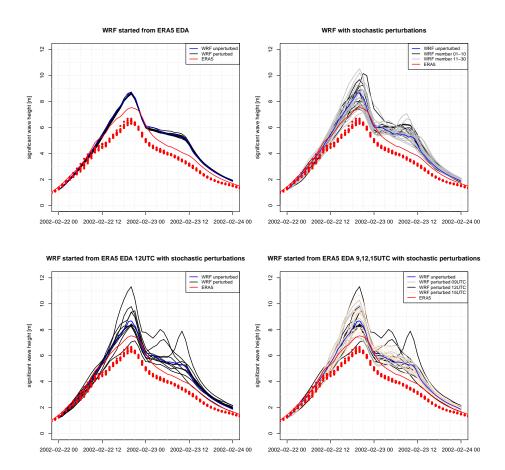
Figure 6. Significant wave height [m] at station Northern Baltic (21.00°E, 59.25°N, see figure 1); driven by WRF ensemble based on initialisations at 2002-02-21 12UTC from ERA5 EDA, ERA5 reanalysis and stochastic perturbations, ERA5 EDA with SKEB and SPPT, and ERA5 EDA with SKEB and SPPT initialed additionally on same day at 09 and 15 UTC; Shown 2002-02-22 21UTC.

wind sea and swell. The later needs some time to travel, so that regions which are predominated by swell can be assumed to need a longer period to produce a reasonable spread with this setting. Osinski et al. (2018) estimated the hundred-year return level of the significant wave height of northerly swell events at the French Guiana coast. Such events are generated in the Northern Atlantic and travel until the north-eastern coast of South America. For hindcasting such events with the demonstrated

5 procedure, a large domain would be necessary and long lasting forecast horizons, so that the waves are already perturbed where generated and over their lifetime as well. This can lead to stronger deviations from the real past state.

3.3 Robustness of the ensemble spread depending on the ensemble size

Each ensemble member is a random draw of the PDF of the forecast / hindcast uncertainty. In the extreme case of having only two members, it is very unlikely that the most extreme cases are represented. By increasing the ensemble size, the probability is

10 getting higher that the full range of uncertainty is sampled. For local area models, operational weather forecast centres produce
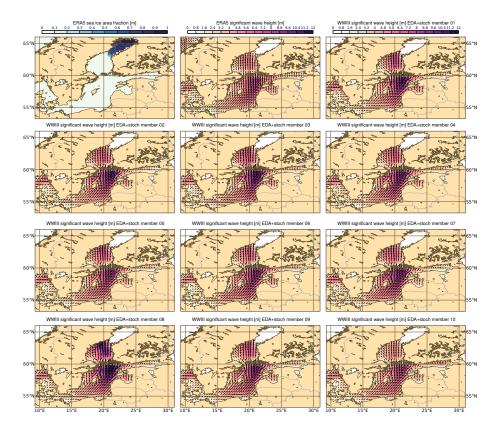
11

Figure 7. ERA5 sea ice area fraction [0-1]; ERA5 significant wave height [m] with direction in meteorological convention and ten Wavewatch III® members driven by WRF ensemble initialised from ten ERA5 EDA members at 2002-02-21 12UTC with SPPT and SKEB. Shown 2002-02-22 21UTC.

ensembles with around ten to twenty members. At first sight, this number seems to be comparable to the presented study. If driving the regional model from a global ensemble with about 30 to 50 ensemble members, one can use a clustering technique to identify the most representative members instead of randomly selecting a small subsample, what improves the ensemble performance (e.g. Nuissier et al., 2012). If the ensemble is initialised several times per day, the different runs can be combined using the LAF approach (e.g. Raynaud and Bouttier, 2017). To predict the probability of the exceedance of a certain threshold, one can apply also neighbourhood techniques (e.g. Theis et al., 2005) or apply post-processing techniques like Bayesian Model Averaging (Raftery et al., 2005). Neither the initial and lateral boundary conditions come from a large ensemble in this study nor the application of neighbourhood or other post-processing techniques helps, because the ensemble members are used to drive a wave model. To get an idea how many ensemble members are reasonable in this case, 500 members have been generated with stochastic perturbations. From these 500 members, an ensemble with N members is generated, with N starting at 10 going until 300. Ten million samples of each ensemble of size N are selected by randomly choosing N out of the 500 members. The standard deviation is used as a measure for the ensemble spread and is calculated for each of the ten million samples of the ensemble of size N. Selecting N out of 500 members, 500 choose N possibilities exist. This number is largely above ten
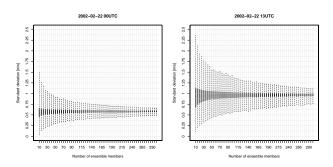
Figure 8. Box-whisker plots of the standard deviation of the 10 m wind speed at 19.39°E, 56.17°N of ten million samples of ensembles of size 10 to 300 randomly sampled from an ensemble with 500 members generated with WRF by applying SKEB and SPPT; shown 2002-02-22 00 and 13UTC. Compare Fig. 2.

millions for all tested ensemble sizes between 10 and 300. If the ensemble size is reasonable to get a robust estimate of the uncertainty, the spread should be relatively similar between each of the samples. Figure 8 shows box-whisker plots for the ten million samples for ensemble sizes between 10 and 300 members.

The variation of the spread in the ten million samples twelve hours after initialisation is demonstrated in the left panel.
5 As it needs some time that the stochastic perturbations provoke spread between the ensemble members, there is a lead time dependence in the spread. The right panel presents a situation 25 hours after initialisation. At this time, the wind speed is very high, see Figure 2. In extreme situations, in which we are especially interested, we expect an higher uncertainty. This higher uncertainty is represented by a larger spread. All the ensembles with sizes between fifteen and hundred members show a median of the spread around one, at February 22nd, 13 UTC. The ten member ensemble has a slightly lower median. With a
10 higher uncertainty, a larger number of ensemble members is necessary to sample the entire uncertainty range. By increasing the ensemble size, the estimation of the uncertainty is getting more robust, why the range of the box-whisker plots is decreasing with increasing ensemble size. At February 22nd, 00 UTC, the uncertainty is lower and / or the spread as a measure of uncertainty is not yet fully developped after twelve hours, why the range of the box-whisker plots is much inferior than thirteen hours later. To achieve a general statement about the ensemble size / spread relation, a much larger sample over a longer
15 period must be investigated, but it can already be concluded that an ensemble size of only ten randomly generated members, as demonstrated in this application, can lead to a significant over- or underestimation of the uncertainty. A compromise between the robustness of the uncertainty estimate and the computational effort has to be found.

3.4 Impact of the spatiotemporal resolution of the atmospheric forcing onto the significant wave height

The time step of a high resolution ocean or wave model is normally below one hour. A higher temporal resolution of atmo-
20 spheric forcing data than one hour is normally not available, but atmospheric forcing fields are needed for all model timesteps. These can be produced for example by linear interpolation in time. If a variable in the ocean-/wave model to be driven has a short response time (e.g. surface current generated by wind compared to SST whose response is slower), and the variability of
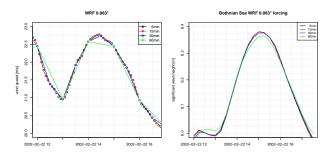
Figure 9. Wind speed [m/s] in 0.063° setup and significant wave height [m] at 20.23°E and 61.8°N ; Testcase without sea ice

the atmospheric forcing in between the temporal resolution of the forcing fields is high, the result can be an under- or overestimation and a erroneous time evolution. One imaginable solution is to use maximum values during the output time interval of the atmospheric model, but this can lead to spatially inconsistent fields, especially if the time interval is very long. To test the impact of different temporal resolutions on the significant wave height, wind fields in 5 minutes resolution were produced with

5   the 0.063° setup. Figure 9 shows the wind field in 5, 15, 30 and 60 minutes resolution at one specific grid cell and the resulting significant wave height at the same location and time. It can be seen that the wind speed maximum in the 60 minutes resolution is about 0.25 m/s below the maxima of the higher temporal resolutions. The higher temporal resolutions do not differ so much. The effect between the 60 minutes and higher resolved temporal forcing on the significant wave height is relatively low with about 2 cm. Systematic differences cannot be found based on the small sample, but it indicates that the choice of the 15 minutes

10   resolution is a reasonable compromise between a good representation of the extreme values and file size.

A stronger impact can be expected from the spatial resolution of the driving wind fields, because a coarser resolution of the atmospheric model can be assumed to produce lower extreme wind speeds as a grid cell represents the average value over the area it covers. By adapting, for example, the parameter betamax which describes the maximum value of wind-wave coupling, this difference can be compensated for. A better representation of the complex orography of the coastlines in the Baltic sea as

15   well as of the various islands is given by the higher resolved WRF model. For this reason, a difference in the spatial pattern can be assumed. A test with the coarsest and the highest resolutions produced in this study has been conducted. The same parameter sets were used, as a calibration is not possible based on the short period hindcasted with WRF. Figure 10 shows the difference between these two forcings on one timestep in the significant wave height. One grid cell of the coarser WRF setup contains 16 grid cells of the higher resolved setup. Maxima as well as minima were found more extreme in the higher

20   resolution with a higher spatial variability, what explains the higher but also the lower wave heights. It would be interesting to determine the remaining difference in the wave parameters provoked by the atmospheric forcings with different resolutions after a calibration of the wave model, done by applying an automatic and objective calibration procedure like for example the one proposed by Gorman and Oliver (2018).
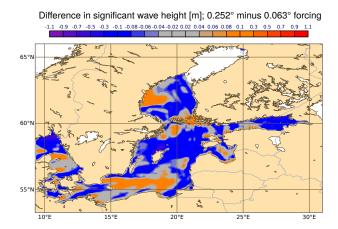
Difference in significant wave height [m]; 0.252° minus 0.063° forcing

Figure 10. Difference in the significant wave height [m] in WAVEWATCH III® between simulation driven by WRF with 0.252° and by 0.063° in 15 minutes temporal resolution at 2002-02-22 21UTC. Part of the Gulf of Bothnia contains sea ice cover fractions above 0.5 why there are no waves.

4 Conclusions

Different approaches for hindcasting a single storm event in the Baltic Sea, which provoked a severe storm surge in February 2002, were tested in this study to create an ensemble hindcast of atmospheric (wind) and wave conditions based on a state-of-the-art atmospheric mesoscale model and a third generation wave model. The objective of the ensemble approach is a
5   quantification of the uncertainty of the hindcast. A lagged-average WRF forecast ensemble showed only little spread with initial and lateral boundary conditions based entirely on the high resolution ERA5 reanalysis fields. The spread of the LAF ensemble can not be easily adapted.[14]

A domain shifting approach with ERA5, in which the input fields are shifted into all directions by one grid cell, shows a more or less comparable spread to the LAF ensemble, with the same advantage of using the high resolution reanalysis data
10   only. The number of ensemble members and the spread of the ensemble is limited to the number of reasonable shifts. Too large shifts can be expected to degrade the hindcast.[15]

Starting WRF from the ERA5 EDA members show also a comparable spread as with the two other approaches. The disadvantage is the coarser resolution of the initial fields. Fine scales are not present in these fields so that the ensemble spread is

---

[14] A weighting of the different realisations (in this case of the wave model) by giving the runs more weight which are expected to have a lower error is possible. In this case more weight to the runs should be given which have smaller errors in the verification of a large sample of hindcasts (e.g. more weight to runs with lower lead time to the desired event), but this can be expected to not strongly enlarge the ensemble spread.

[15] As the WRF model has a finer resolution, shifts different than multiples of one grid cell by adding or substracting an offset onto the coordinates of the ERA5 grid would change the interpolation for the WRF initial and lateral boundary conditions. This was not tested, and it was also not investigated systematically if members generated from smaller shifts are closer to the unpertubed run or if shifts into a certain direction (e.g. into flow direction or perpendicular to it) lead to different spreads than shifts into other directions, which would mean that there are systematic differences between the members to be taken into account by the interpretation of the ensemble data. A test with shifts of two and three grid cells into north, west, south and east direction were tested and indicate that there are systematic differences.

limited by this fact. Stochastic perturbations produce a much larger spread, but need some time to develop. As the first twelve hours are not used, because of the model spin-up, this is not really a shortcoming. A combination of stochastic pertubations and an initialisation from the ERA5 EDA fields produces also deviations from the unperturbed runs which are not present by only using the stochastic perturbations. This approach is especially interesting and is close to what is used in meterological

5   weather forecast centres for the operational forecasts. The wind fields from this ensemble hindcast produce also a large spread in the wave model. A visual comparison with the ERA5 wave model ensemble of data assimilations indicates that this spread is more reasonable than using the first three discussed ensemble generation approaches.

    The robustness of the spread depending on the ensemble size was tested by randomly generating ensembles with different sizes (10 to 300 members) from an ensemble hindcast with 500 members. For small ensembles, the range of the ensemble

10   spread can differ largely depending which members were randomly selected. In operational services, this problem is tackled by selecting for example already representative members from a larger global ensemble. To achieve a comparable robust estimate of the uncertainty, the ensemble size for the here presented approach must be larger than the one of operational local area model ensembles.

    Another source of uncertainty arises from the spatiotemporal discretisation of the atmopsheric model and the resulting

15   forcing fields for the wave model. Errors introduced by a coarse temporal resolution of the driving wind fields in the significant wave height are relatively small in this event testcase. For a strong event, the difference between a 5 and 60 minutes temporally resolved wind forcing is only on the order of 2 cm. Between 15 minutes and 5 minutes temporal resolution, the impact on the wave height is negligible for the demonstrated case. The horizontal resolution has a much stronger impact. This can be potentially be corrected by calibrating the model to the different wind forcings. It would be interesting to estimate the

20   remaining difference, but this was not possbile in the framework of this study as a calibration of the models is not feasible based on a hindcast of only a single event.

    A combination of ERA5 EDA fields as initial conditions and the stochastic perturbations showed the ability to produce a larger spread than with the other demonstrated approaches. Stochastic perturbations haven't been tuned in this study. Producing longer timeseries, for tuning and validating the model could lead to a reasonable measure of the hindcast uncertainty on the

25   regional scale and allows to adapt the spatiotemporal resolution and number of members to the applications needs.

Code availability. The WRF source code is available from https://github.com/wrf-model/WRF/releases and the Wavewatch III[®] from https://github.com/NOAA-EMC/WW3

Data availability. ERA5 and the UERRA/Harmonie-v1 reanalysis can be retrieved from the Climate data store at https://cds.climate.copernicus.eu.

Sample availability. Ensemble hindcasts of wind and wave fields presented in this study can be requeested by contacting the corresponding author.

Author contributions. RDO is responsible for the concept of this study, prepared the configurations of WRF and Wavewatch III®, conducted the simulations and prepared the presentation of the results. HR was involved in the discussion of the results and in the preparation of the

5 manuscript.

Competing interests. The authors declare that there is no conflict of interest.

References

Ardhuin, F., H C Herbers, T., O'Reilly, W., and Jessen, P.: Swell Transformation across the Continental Shelf. Part I: Attenuation and Directional Broadening, Journal of Physical Oceanography, 33, 1921, https://doi.org/10.1175/1520-0485(2003)033<1921:STATCS>2.0.CO;2, 2003.

5 Ardhuin, F., Rogers, E., Babanin, A. V., Filipot, J.-F., Magne, R., Roland, A., van der Westhuysen, A., Queffeulou, P., Lefevre, J.-M., Aouf, L., and Collard, F.: Semiempirical Dissipation Source Functions for Ocean Waves. Part I: Definition, Calibration, and Validation, Journal of Physical Oceanography, 40, 1917–1941, https://doi.org/10.1175/2010JPO4324.1, https://doi.org/10.1175/2010JPO4324.1, 2010.

Bouttier, F., Vié, B., Nuissier, O., and Raynaud, L.: Impact of Stochastic Physics in a Convection-Permitting Ensemble, Monthly Weather Review, 140, 3706–3721, https://doi.org/10.1175/MWR-D-12-00031.1, https://doi.org/10.1175/MWR-D-12-00031.1, 2012.

10 Brankart, J.-M., Candille, G., Garnier, F., Calone, C., Melet, A., Bouttier, P.-A., Brasseur, P., and Verron, J.: A generic approach to explicit simulation of uncertainty in the NEMO ocean model, Geoscientific Model Development, 8, 1285–1297, https://doi.org/10.5194/gmd-8-1285-2015, https://www.geosci-model-dev.net/8/1285/2015/, 2015.

Buizza, R.: Impact of Horizontal Diffusion on T21, T42, and T63 Singular Vectors, Journal of the Atmospheric Sciences, 55, 1069–1083, https://doi.org/10.1175/1520-0469(1998)055<1069:IOHDOT>2.0.CO;2, https://doi.org/10.1175/1520-0469(1998)055<1069:IOHDOT>
15 2.0.CO;2, 1998.

Buizza, R., Milleer, M., and Palmer, T. N.: Stochastic representation of model uncertainties in the ECMWF ensemble prediction system, Quarterly Journal of the Royal Meteorological Society, 125, 2887–2908, https://doi.org/10.1002/qj.49712556006, https://rmets.onlinelibrary.wiley.com/doi/abs/10.1002/qj.49712556006, 1999.

Buizza, R., Leutbecher, M., and Isaksen, L.: Potential use of an ensemble of analyses in the ECMWF Ensemble Prediction System, Quarterly
20 Journal of the Royal Meteorological Society, 134, 2051–2066, https://doi.org/10.1002/qj.346, https://rmets.onlinelibrary.wiley.com/doi/abs/10.1002/qj.346, 2008.

Copernicus Climate Change Service (C3S): ERA5: Fifth generation of ECMWF atmospheric reanalyses of the global climate. Copernicus Climate Change Service Climate Data Store (CDS), accessed on 26th march 2019, https://cds.climate.copernicus.eu/cdsapp#!/home, 2017.

ECMWF: Part VII: ECMWF Wave Model, no. 7 in IFS Documentation, ECMWF, https://www.ecmwf.int/node/16651, 2016.

25 Farina, L.: On ensemble prediction of ocean waves, Tellus A, 54, 148–158, https://doi.org/10.1034/j.1600-0870.2002.01301.x, https://onlinelibrary.wiley.com/doi/abs/10.1034/j.1600-0870.2002.01301.x, 2002.

Gorman, R. M. and Oliver, H. J.: Automated model optimisation using the Cylc workflow engine (Cyclops v1.0), Geoscientific Model Development, 11, 2153–2173, https://doi.org/10.5194/gmd-11-2153-2018, https://www.geosci-model-dev.net/11/2153/2018/, 2018.

Hagedorn, R., Doblas-Reyes, F. J., and Palmer, T. N.: The rationale behind the success of multi-model ensembles in seasonal forecasting
30 – I. Basic concept, Tellus A, 57, 219–233, https://doi.org/10.1111/j.1600-0870.2005.00103.x, https://onlinelibrary.wiley.com/doi/abs/10.1111/j.1600-0870.2005.00103.x, 2005.

Hamill, T. M.: Interpretation of Rank Histograms for Verifying Ensemble Forecasts, Monthly Weather Review, 129, 550–560, https://doi.org/10.1175/1520-0493(2001)129<0550:IORHFV>2.0.CO;2, https://doi.org/10.1175/1520-0493(2001)129<0550:IORHFV>
2.0.CO;2, 2001.

35 Hoffman, R. N. and Kalnay, E.: Lagged average forecasting, an alternative to Monte Carlo forecasting, Tellus A, 35A, 100–118, https://doi.org/10.1111/j.1600-0870.1983.tb00189.x, https://onlinelibrary.wiley.com/doi/abs/10.1111/j.1600-0870.1983.tb00189.x, 1983.

Jolliffe, I. T. and Stephenson, D. B.: Forecast Verification: A Practitioner's Guide in Atmospheric Science, John Wiley & Sons Ltd.: Chichester, UK., 2003.

Leutbecher, M., Lock, S.-J., Ollinahob, P., Lang, S. T. K., Balsamo, G., Bechtold, P., Bonavita, M., Christensenc, H. M., Diamantakis, M., Dutra, E., English, S., Fisher, M., Forbes, R. M., Goddard, J., Haiden, T., Hogan, R. J., Jurickec, S., Lawrence, H., MacLeodc, D.,
5   Magnusson, L., Malardel, S., Massart, S., Sandu, I., Smolarkiewicz, P. K., Subramanianc, A., Vitart, F., Wedi, N., and Weisheimer, A.: Stochastic representations of modeluncertainties at ECMWF:State of the art and future vision, Tech. rep., European Centre for Medium-Range Weather Forecasts, Shinfield Park, Reading, RG2 9AX, England, 2016.

Leutbecher, M., Lock, S.-J., Ollinaho, P., Lang, S. T. K., Balsamo, G., Bechtold, P., Bonavita, M., Christensen, H. M., Diamantakis, M., Dutra, E., English, S., Fisher, M., Forbes, R. M., Goddard, J., Haiden, T., Hogan, R. J., Juricke, S., Lawrence, H., MacLeod, D., Magnusson,
10   L., Malardel, S., Massart, S., Sandu, I., Smolarkiewicz, P. K., Subramanian, A., Vitart, F., Wedi, N., and Weisheimer, A.: Stochastic representations of model uncertainties at ECMWF: state of the art and future vision, Quarterly Journal of the Royal Meteorological Society, 143, 2315–2339, https://doi.org/10.1002/qj.3094, https://rmets.onlinelibrary.wiley.com/doi/abs/10.1002/qj.3094, 2017.

Lorenz, E. N.: Deterministic Nonperiodic Flow, Journal of the Atmospheric Sciences, 20, 130–141, https://doi.org/10.1175/1520-0469(1963)020<0130:DNF>2.0.CO;2, https://doi.org/10.1175/1520-0469(1963)020<0130:DNF>2.0.CO;2, 1963.

15 Murphy, A. H. and Winkler, R. L.: Diagnostic verification of probability forecasts, International Journal of Forecasting, 7, 435–455, https://EconPapers.repec.org/RePEc:eee:intfor:v:7:y:1992:i:4:p:435-455, 1992.

Nuissier, O., Joly, B., Vié, B., and Ducrocq, V.: Uncertainty of lateral boundary conditions in a convection-permitting ensemble: a strategy of selection for Mediterranean heavy precipitation events, Natural Hazards and Earth System Sciences, 12, 2993–3011, https://doi.org/10.5194/nhess-12-2993-2012, https://www.nat-hazards-earth-syst-sci.net/12/2993/2012/, 2012.

20 Ollinaho, P., Lock, S.-J., Leutbecher, M., Bechtold, P., Beljaars, A., Bozzo, A., Forbes, R. M., Haiden, T., Hogan, R. J., and Sandu, I.: Towards process-level representation of model uncertainties: stochastically perturbed parametrizations in the ECMWF ensemble, Quarterly Journal of the Royal Meteorological Society, 143, 408–422, https://doi.org/10.1002/qj.2931, https://rmets.onlinelibrary.wiley.com/doi/abs/10.1002/qj.2931, 2017.

Osinski, R., Lorenz, P., Kruschke, T., Voigt, M., Ulbrich, U., Leckebusch, G. C., Faust, E., Hofherr, T., and Majewski, D.: An approach
25   to build an event set of European windstorms based on ECMWF EPS, Natural Hazards and Earth System Sciences, 16, 255–268, https://doi.org/10.5194/nhess-16-255-2016, https://www.nat-hazards-earth-syst-sci.net/16/255/2016/, 2016.

Osinski, R., Dalphinet, A., Aouf, L., and Palany, P.: Estimation of the hundred year return level of the significant wave height for the French Guiana coast, Brazilian Journal of Oceanography, 66, 325 – 334, http://www.scielo.br/scielo.php?script=sci_arttext&pid=S1679-87592018000400325&nrm=iso, 2018.

30 Pardowitz, T., Befort, D. J., Leckebusch, G. C., and Ulbrich, U.: Estimating uncertainties from high resolution simulations of extreme wind storms and consequences for impacts, Meteorologische Zeitschrift, 25, 531–541, https://doi.org/10.1127/metz/2016/0582, http://dx.doi.org/10.1127/metz/2016/0582, 2016.

Peckham, S. E., Smirnova, T. G., Benjamin, S. G., Brown, J. M., and Kenyon, J. S.: Implementation of a Digital Filter Initialization in the WRF Model and Its Application in the Rapid Refresh, Monthly Weather Review, 144, 99–106, https://doi.org/10.1175/MWR-D-15-
35   0219.1, https://doi.org/10.1175/MWR-D-15-0219.1, 2016.

Raftery, A. E., Gneiting, T., Balabdaoui, F., and Polakowski, M.: Using Bayesian Model Averaging to Calibrate Forecast Ensembles, Monthly Weather Review, 133, 1155–1174, https://doi.org/10.1175/MWR2906.1, https://doi.org/10.1175/MWR2906.1, 2005.

Raynaud, L. and Bouttier, F.: The impact of horizontal resolution and ensemble size for convective-scale probabilistic forecasts, Quarterly Journal of the Royal Meteorological Society, 143, 3037–3047, https://doi.org/10.1002/qj.3159, https://rmets.onlinelibrary.wiley.com/doi/abs/10.1002/qj.3159, 2017.

Ricchi, A., Miglietta, M. M., Bonaldo, D., Cioni, G., Rizza, U., and Carniel, S.: Multi-Physics Ensemble versus Atmosphere–Ocean Coupled Model Simulations for a Tropical-Like Cyclone in the Mediterranean Sea, Atmosphere, 10, https://doi.org/10.3390/atmos10040202, http://www.mdpi.com/2073-4433/10/4/202, 2019.

Ridal, M., Olsson, E., Unden, P., Zimmermann, K., and Ohlsson, A.: Uncertainties in Ensembles of Regional Re-Analyses - Deliverable D2.7 HARMONIE reanalysis report of results and dataset, http://www.uerra.eu/component/dpattachments/?task=attachment.download&id=296, 2017.

Seifert, T., Tauber, F., and Kayser, B.: A high resolution spherical grid topography of the Baltic Sea - 2nd edition, in: Baltic Sea Science Congress, Stockholm 25-29, Poster No. 147, www.io-warnemuende.de/iowtopo, 2001.

Shutts, G.: A kinetic energy backscatter algorithm for use in ensemble prediction systems, Quarterly Journal of the Royal Meteorological Society, 131, 3079–3102, https://doi.org/10.1256/qj.04.106, https://rmets.onlinelibrary.wiley.com/doi/abs/10.1256/qj.04.106, 2005.

Skamarock, W. C., Klemp, J. B., Dudhia, J., Gill, D. O., Liu, Z., Berner, J., Wang, W., Powers, J. G., Duda, M. G., Barker, D., and yu Huang, X.: A Description of the Advanced Research WRF Model Version 4, Tech. rep., NCAR/TN-556+STR, https://doi.org/doi:10.5065/1dfh-6p97, 2019.

Swinbank, R., Kyouda, M., Buchanan, P., Froude, L., Hamill, T. M., Hewson, T. D., Keller, J. H., Matsueda, M., Methven, J., Pappenberger, F., Scheuerer, M., Titley, H. A., Wilson, L., and Yamaguchi, M.: The TIGGE Project and Its Achievements, Bulletin of the American Meteorological Society, 97, 49–67, https://doi.org/10.1175/BAMS-D-13-00191.1, https://doi.org/10.1175/BAMS-D-13-00191.1, 2016.

The WAVEWATCH III® Development Group (WW3DG): User manual and system documentation of WAVEWATCH III® version 6.07. Tech. Note 333, 2019.

Theis, S. E., Hense, A., and Damrath, U.: Probabilistic precipitation forecasts from a deterministic model: a pragmatic approach, Meteorological Applications, 12, 257–268, https://doi.org/10.1017/S1350482705001763, https://rmets.onlinelibrary.wiley.com/doi/abs/10.1017/S1350482705001763, 2005.

Tolman, H. L.: A Third-Generation Model for Wind Waves on Slowly Varying, Unsteady, and Inhomogeneous Depths and Currents, Journal of Physical Oceanography, 21, 782–797, https://doi.org/10.1175/1520-0485(1991)021<0782:ATGMFW>2.0.CO;2, https://doi.org/10.1175/1520-0485(1991)021<0782:ATGMFW>2.0.CO;2, 1991.

Toth, Z. and Kalnay, E.: Ensemble Forecasting at NCEP and the Breeding Method, Monthly Weather Review, 125, 3297–3319, https://doi.org/10.1175/1520-0493(1997)125<3297:EFANAT>2.0.CO;2, https://doi.org/10.1175/1520-0493(1997)125<3297:EFANAT>2.0.CO;2, 1997.

Wang, W., Bruyère, C., Duda, M., Dudhia, J., Gill, D., Kavulich, M., Werner, K., Chen, M., Lin, H.-C., Michalakes, J., Rizvi, S., Zhang, X., Berner, J., Munoz-Esparza, D., Reen, B., and Fossel, S. H. K.: User's Guide for the Advanced Research WRF (ARW) Modeling System, Version 4, http://www2.mmm.ucar.edu/wrf/users/docs/user_guide_V4/WRFUsersGuide.pdf, 2019.

Yildirim, B. and Karniadakis, G. E.: Stochastic simulations of ocean waves: An uncertainty quantification study, Ocean Modelling, 86, 15 – 35, https://doi.org/https://doi.org/10.1016/j.ocemod.2014.12.001, http://www.sciencedirect.com/science/article/pii/S1463500314001759, 2015.